Histol Histopathol (2023) 38: 585-595

http://www.hh.um.es

Histology and Histopathology
From Cell Biology to Tissue Engineering

ORIGINAL ARTICLE **Open Access**

Circular RNA hsa_circ_0003892 promotes the development of papillary thyroid carcinoma by regulating the miR-326/LASP1 axis

Peng Han, Junsong Liu, Qian Zhao, Honghui Li, Ting Zhang, Baiya Li and Xiaorong Niu

Department of Otorhinolaryngology-Head and Neck Surgery, the First Affiliated Hospital of Xi'an Jiaotong University, Xi'an, Shaanxi, PR China

Summary. Background. Thyroid cancer is the most common malignancy of the endocrine system. Circular RNA (circRNA) is recognized as a key regulator of tumorigenesis in papillary thyroid carcinoma (PTC). Here this work focused on the mechanism of circRNA_0003892 (circ_0003892) in PTC progression.

Methods. Quantitative real-time polymerase chain reaction (qRT-PCR) was used to examine circ_0003892, microRNA-326 (miR-326) and LIM and SH3 protein 1 (LASP1) mRNA expression levels in PTC tissues and cell lines. Besides, cell counting kit-8 (CCK-8), EdU and transwell assays were conducted to detect the proliferative, migrative and invasive abilities of PTC cells, respectively. B The targeting relationships between miR-326 and circ_0003892 or LASP1 3'-UTR were verified by dual-luciferase reporter gene assay and RNA immunoprecipitation (RIP) assay.

Results. Circ_0003892 expression was raised in PTC tissues and cells, which was significantly interrelated with larger tumor size and extrathyroidal extension in PTC sufferers. Overexpression of circ_0003892 significantly promoted the malignant biological behaviors of PTC cells. Additionally, miR-326 was a downstream target of circ_0003892, and miR-326 overexpression weakened the promoting effect of circ_0003892 overexpression on the malignant progression of PTC. MiR-326 specifically inhibited LASP1. Circ_0003892 positively regulated LASP1 expression by targeting miR-326.

Conclusion. Circ_0003892 up-regulates LASP1 expression and facilitates PTC progression via competitively binding to miR-326.

Corresponding Author: Xiaorong Niu, Department of Otorhinolaryngology-Head and Neck Surgery, the First Affiliated Hospital of Xi'an Jiaotong University, Xi'an 710061, Shaanxi, China. e-mail: vvk493647@163.com

DOI: 10.14670/HH-18-546

Key words: Papillary thyroid carcinoma, circ_0003892, miR-326, LASP1

Introduction

Papillary thyroid carcinoma (PTC) is a common endocrine malignancy, which accounts for about 85% of all follicular cell-derived thyroid cancers (Coca-Pelaz et al., 2020). At present, comprehensive treatment including thyroidectomy, radioiodine, and thyroid-stimulating hormone suppression therapy may work, with a 5-year survival rate of more than 95% (Yin et al., 2017). Although most PTCs are well differentiated with low rates of local invasion, recurrence, or metastasis, a small percentage of tumors still exhibit heterogeneity with more aggressive properties, which leads to unfavorable prognosis (Haugen et al., 2016; Ge et al., 2017). Hence it is vital to expound the underlying molecular mechanisms of carcinogenesis and progression of PTC to further improve the clinical treatment of PCT.

Circular RNAs (circRNAs) are endogenous non-coding RNA transcripts, which possess a covalent loop structure and thus are stable, abundant, and conserved (Wang et al., 2016). CircRNAs were previously considered as "junk" without any biological functions (Patop et al., 2019). However in recent years, it is reported that circRNAs are implicated in diverse physiological and pathological processes (Li et al., 2018, 2020), especially in tumorigenesis (Liu et al., 2019; Yao et al., 2019; Gong et al., 2021). For instance, circ_0058124, as an oncogenic factor, facilitates the growth and invasion of PTC cells (Yao et al., 2019). In this study, we proved by bioinformatics analysis that

Abbreviations. PTC, Papillary thyroid carcinoma (PTC); circRNAs, Circular RNAs; miRNAs, MicroRNAs; LASP1, LIM and SH3 protein 1; qRT-PCR, quantitative real-time polymerase chain reaction; WT, Wild-type (WT); MUT, mutant.

circ_0003892 expression was elevated in PTC tissues. However, its function and mechanism in PTC progression have not yet been elucidated.

MicroRNAs (miRNAs) are small non-coding RNAs of about 21*nt* that are involved in the post-transcriptional regulation of target genes (Krol et al., 2010; Chen et al., 2019). MiRNAs act as oncogenes or tumor suppressors via targeting and regulating different mRNAs (Svoronos et al., 2016; Jin et al., 2019). MiR-326 expression is inhibited in PTC tissues and miR-326 restrains the growth, migration and invasion of PTC cells by targeting MAPK1 and ERBB4 (Nie et al, 2020). Instead, the mechanism of miR-326 dysregulation in PTC has not been fully elucidated.

In this work, we investigated the expression characteristics and functions of circ_0003892 in PTC and focused on its potential molecular mechanisms. We observed that circ_0003892 expression was up-regulated in PTC tissues and cells, and this change facilitated the proliferative, migrative, and invasive abilities of PTC cell by regulating the miR-326/LIM and SH3 protein 1 (LASP1) axis. This study deepens the understanding of the pathogenesis of PTC and potentially delivers new ideas for improving the clinical treatment of PTC.

Materials and methods

Ethics statement and tissue samples

PTC tumor tissues and normal tissues were available from 56 PTC patients who received surgical resection in the First Affiliated Hospital of Xi'an Jiaotong University between December 2016 and October 2019. All participants did not receive radiotherapy or chemotherapy before tissue sample collection. Immediately after surgical excision, the tissue samples were frozen in liquid nitrogen and kept at -80°C. This work, with written informed consent, was endorsed by the Ethics Committee of the First Affiliated Hospital of Xi'an Jiaotong University.

Cell Culture and transfection

Human thyroid carcinoma cell lines K1, IHH-4, BCPAP and TCP-1, human thyroid follicular epithelial cells Nthy-ori 3-1, and human embryonic kidney cells HEK-293T were available from the American Type Culture Collection (Rockville, MD, USA). These cells were cultured in Dulbecco's modified Eagle's medium (Hyclone, Logan, UT, USA) with 10% fetal bovine serum (FBS, Sigma, St. Louis, MO, USA), 100 U/ml penicillin and 100 μg/ml streptomycin (Invitrogen, Carlsbad, CA, USA) at 37°C in 5% CO_2. The cells were routinely subcultured with 0.25% trypsin (Roche, Basel, Swizerland) when they reached 70% to 80% confluence.

Circ_0003892 overexpression plasmid vector (circ_0003892-OE), empty vector (NC), miR-326 mimics and its control (mimNC) were generally constructed by GenePharma (Shanghai, China). The above plasmids and oligonucleotides (50 nM) were subsequently transfected into IHH-1 and TCP-1 cells with Lipofectamine® 3000 (Invitrogen) according to the manufacturer's instructions. 24h later, the cells were collected. Ultimately, the transfection efficacy was measured by quantitative real-time polymerase chain reaction (qRT-PCR).

qRT-PCR

Total RNA from tissues and cells was accordingly extracted by TRIzol reagent (Invitrogen). 500 ng of RNA was reversely transcribed into cDNA with the SuperScript First-Stand Synthesis system (Invitrogen). Next, qRT-PCR was performed with a SYBR Select Master Mix kit (Applied Biosystems, Foster City, CA, USA) on an ABI73900 system (Applied Biosystems, Foster City, CA, USA) according to the manufacturer's instructions. The relative expression levels of the genes were calculated with $2^{-\Delta\Delta Ct}$ method, with U6 and GAPDH as internal references. The specific primer sequences are: Circ_0003892 Forward: 5'-ATAG TGACAATGTCTCACC-3'; Circ_0003892 Reverse: 5'-GACAAAGTATTTTGGACAG-3'; MiR-326 Forward: 5'-CATCTGTCTGTTGGGCTGGA -3' MiR-326 Reverse: 5'-AGGAAGGGCCCAGAGGCG -3' LASP1 Forward: 5'-TGCGGCAAGATCGTGTATCC-3' LASP1 Reverse: 5'-GCAGTAGGGCTTCTCGTAG-3' U6 Forward: 5 '-CTCGCTTCGGCAGCACATATACT-3', U6 Reverse: 5'-ACGCTTCACGAATTTGCGTGTC-3'; GAPDH Forward: 5'-TACCCCCAATGTGTCCGTC-3', GAPDH Reverse: 5'-GCCCAAGATGCCCTTCAGT-3'.

Subcellular localization analysis

Subcellular localization analysis of RNA was performed with a PARIS™ kit (Thermo Fisher Scientific, Waltham, MA, USA). IHH-4 and TCP-1 cells were re-suspended with cell isolation buffer, and subsequently the cytoplasmic fraction and nuclear fraction of the cells were isolated, and the cytoplasmic RNA and nuclear RNA were extracted, respectively. The expression of circ_0003892 in the cytoplasm and nucleus of the cells was then detected by qRT-PCR, with GAPDH and U6 as cytoplasmic or nuclear controls, respectively.

Cell counting kit-8 (CCK-8) assay

IHH-4 and TCP-1 cells were inoculated in 96-well plates at the density of 2×10^3/well and cultured for 24h at 37°C. Next, the cells were incubated with 10 μL of CCK-8 solution (Dojindo Molecular Technologies, Japan) for 1h at 37°C. After the culture was terminated, the value of OD450 nm was estimated by a microplate reader.

EdU assay

Cell viability was probed by the EdU kit (Beyotime

Biotechnology, Shanghai, China). IHH-4 and TCP-1 cells were inoculated in 24-well plates at the density of 2.5×10^5 cells/well and then cultured for 24h at 37°C. 200 μL of EdU solution (Beyotime Biotechnology, Shanghai, China) at a final concentration of 50 μM was loaded into each well and accordingly incubated with the cells for 2h at 37°C. Then, the cells were washed with phosphate buffer saline (PBS), and subsequently fixed with paraformaldehyde and mixed with 200 μL of glycine (final concentration of 2 mg/mL), and incubated for 5 min on a shaker. Next, cells were loaded with 0.5% TritonX-100 in PBS for 10 min, stained with Apollo for 30 min and then incubated with DAPI staining solution for 20 min at ambient temperature in the dark. Next, the cells were rinsed with PBS and photographed, with the numbers of cells counted under an Olympus BX43F fluorescence microscope (Olympus, Tokyo, Japan).

Transwell assay

Transwell assays were performed with transwell inserts (Costar, Cambridge, MA, USA) to detect the migrative and invasive abilities of PTC cells. About 5×10^4 cells were suspended in 200 μL of serum-free medium and loaded into the upper chamber of the transwell insert, and the lower chamber was added with 600 μL of medium containing 10% FBS. After 24h of culture at 37°C, the chamber was subsequently removed and cells in the upper chamber were gently wiped off with a cotton swab. Next, the cells on the lower surface of the filter were fixed with 4% paraformaldehyde for 10 min and subsequently stained with 0.1% crystal violet solution for 15 min. Rinsed twice with PBS, the cells were air-dried, and five fields of the filter were randomly taken under an inverted microscope (magnification 200×) for photographing and counting. Inserts with Matrigel (1:10; BDBiosciences, FranklinLakes, NJ, USA) were used for invasion assays, but inserts without Matrigel were used for migration assays.

Dual-reporter luciferase gene assay

Wild-type (WT) luciferase vectors (circ_0003892 WT, LASP1 WT) and mutant (MUT) luciferase vectors (circ_0003892 MUT, LASP1 MUT) were constructed by Promega (Madison, WI, USA). IHH-4 and TCP-1 cells (1×10^5 cells) were plated into 48-well plates and subsequently cultured for 24h at 37°C. Circ_0003892 WT/MUT or LASP1WT/MUT were accordingly co-transfected into IHH-4 and TCP-1 cells with miR-326 mimics or their negative controls by Lipofectamine® 3000 (Invitrogen). Ultimately, the luciferase activity was detected 48h after transfection by the Dual-luciferase reporter gene assay System (Promega).

RNA immunoprecipitation (RIP)

RIP assays were conducted with the Magna RIP RNA-binding protein immunoprecipitation kit (Millipore, Billerica, MA, USA) according to the manufacturer's instructions. IHH-4 and TCP-1 cells were lysed by RIP lysis buffer. 100 μL of whole cell extract was incubated with magnetic beads conjugated with anti-Argonaute 2 (Ago2) antibody (Millipore) or negative control mouse IgG antibody (Millipore) for 8h at 4°C. The beads were immersed in RIP wash buffer, and the immunoprecipitate was subsequently treated with proteinase K for 30 min at 55°C. Ultimately, the immunoprecipitated RNA was extracted and the enrichment of circ_0003892 and miR-326 in the immunoprecipitate was probed by qRT-PCR.

Western blot assay

Total cellular protein was extracted by RIPA lysis buffer (Sigma-Aldrich, Burlington, Massachusetts, USA), with the concentration determined by the bicinchoninic acid (BCA) kit (Thermo, Rockford, IL, USA). The protein samples (20 μg / lane) were separated via sodium dodecyl sulfate polyacrylamide gel electrophoresis (SDS-PAGE) and then transferred onto polyvinylidene fluoride membranes (Millipore, Bedford, MA, USA), which was blocked with 5% skimmed milk for 1h at room temperature, and then washed three times in tris buffered saline tween (TBST). The proteins were incubated with anti-LASP1 antibody (ab156872, 1:1000, Abcam, Shanghai, China) and anti-GAPDH antibody (ab9485, 1:1500, Abcam, Shanghai, China) overnight at 4°C. After rinsing with TBST, the proteins were incubated with Goat Anti-Rabbit IgG (ab205718, 1:5000, Abcam, Shanghai, China) for 1h at ambient

Table 1. The correlation between clinicopathological features and expression of circ_0003892 in papillary thyroid carcinoma.

Pathological Parameters	Numbers (n=56)	Circ_0003892 expression	
		High (n=28)	Low (n=28)
Age (years)			
<45	23	12	11
≥45	33	16	17
Gender			
Male	30	17	13
Famale	26	11	15
Tumor size (cm)			
≥3 cm	30	20	10
<3 cm	26	8	18
Extrathyroidal invasion			
Present	27	18	9
Absent	29	10	19
Nodular Goiter			
Negative	31	16	15
Positive	25	12	13
TNM stage			
I + II	30	13	17
III + IV	26	15	11

*Presents a statistical difference less than 0.05.

temperature. Ultimately, the proteins were visualized and imaged by an enhanced chemiluminescence (ECL) kit (Promega), with GAPDH as an internal reference.

Statistical analysis

All of the experiments were performed in triplicate. The statistical analysis was performed with SPSS 23.0 statistical analysis software (SPSS Inc., Chicago, IL, USA), with data expressed as "mean ± standard deviation". The comparison between two groups was analyzed by Student's t test and the comparison among multiple groups performed by one-way analysis of variance followed by Tukey's post-hoc test. The relationships between circ_0003892 expression and clinicopathological parameters of the PTC patients were analyzed by the chi-square test. Statistically, $P<0.05$ is meaningful.

Results

Circ_0003892 expression is raised in PTC tissues and cell lines

GSE93522 dataset was downloaded from Gene Expression Omnibus (GEO) database and analyzed, and we observed that circ_0003892 expression was up-regulated in PTC tissues (Fig. 1A,B). Besides, qRT-PCR showed that circ_0003892 expression was remarkably up-regulated in PTC tissues and cell lines as against that of adjacent tissues or human thyroid follicular epithelial cells Nthy-ori 3-1 (Fig. 1C,D). Notably, circ_0003892 was mainly distributed in the cytoplasm of IHH-4 and TCP-1 cells (Fig. 1E). Chi-square test showed that the high expression of circ_0003892 was associated with larger tumor size and extrathyroidal invasion of PTC patients (Table 1). Collectively, circ_0003892 may

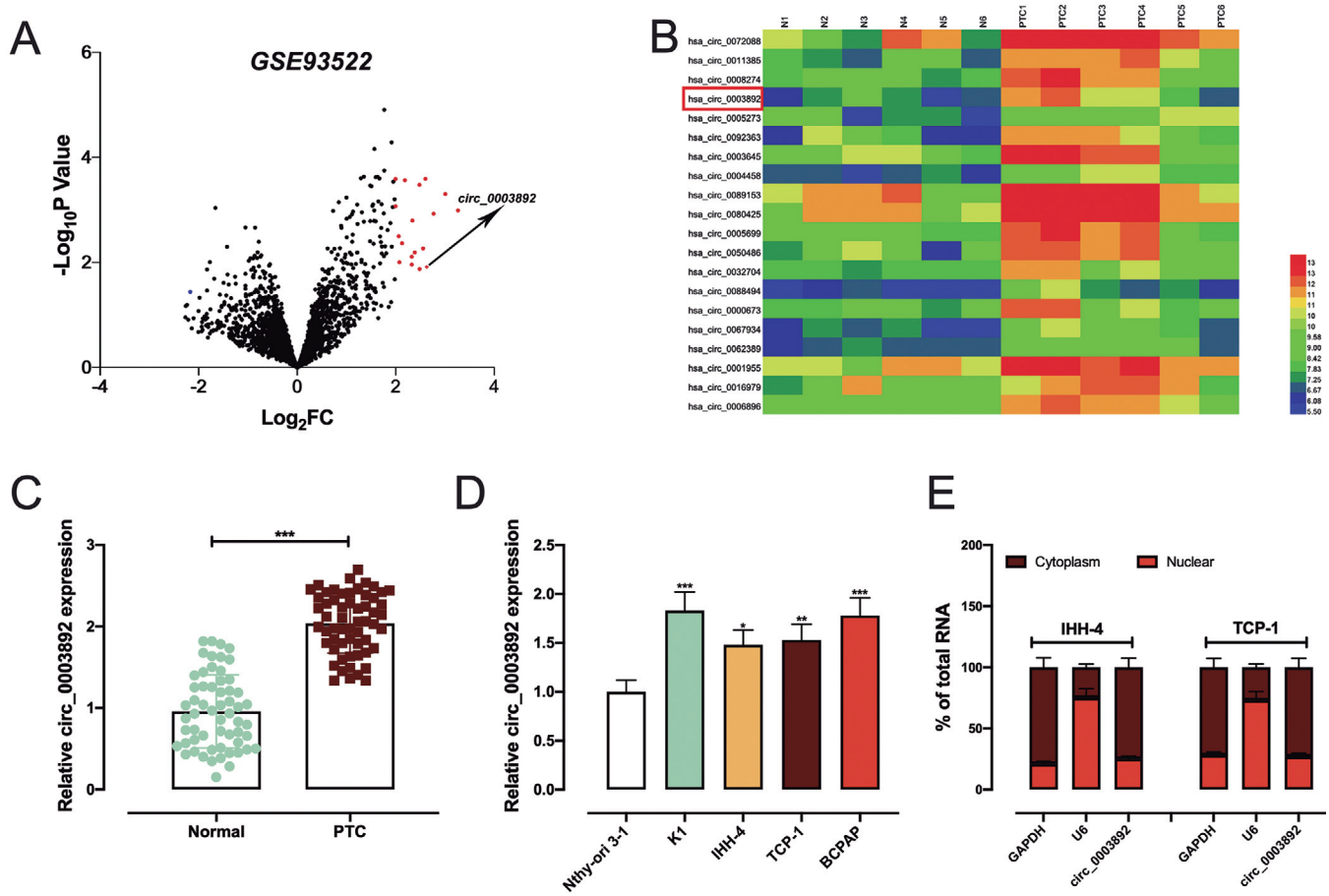

Fig. 1. Circ_0003892 expression is up-regulated in PTC tissues and cell lines. **A.** Volcano plots show the expression differences of circRNAs in the dataset GSE93522 (cutoff criteria: log2 l fold change l>2, and P<0.05), with down-regulated circRNAs marked in blue and up-regulated circRNAs marked in red. Black represents circRNAs without significant change. **B.** Differentially expressed circRNAs in PTC tissues (PTC1-PTC6) and normal tissues (N1-N6) were plotted by a heatmap. **C, D.** qRT-PCR was used to detect circ_0003892 expression in PTC tissues and cell lines. **E.** Nucleocytoplasmic separation assay was used to detect the subcellular localization of circ_0003892 in PTC cells. All of the experiments were performed in triplicate. **P*<0.05, ***P*<0.01 and ****P*<0.001.

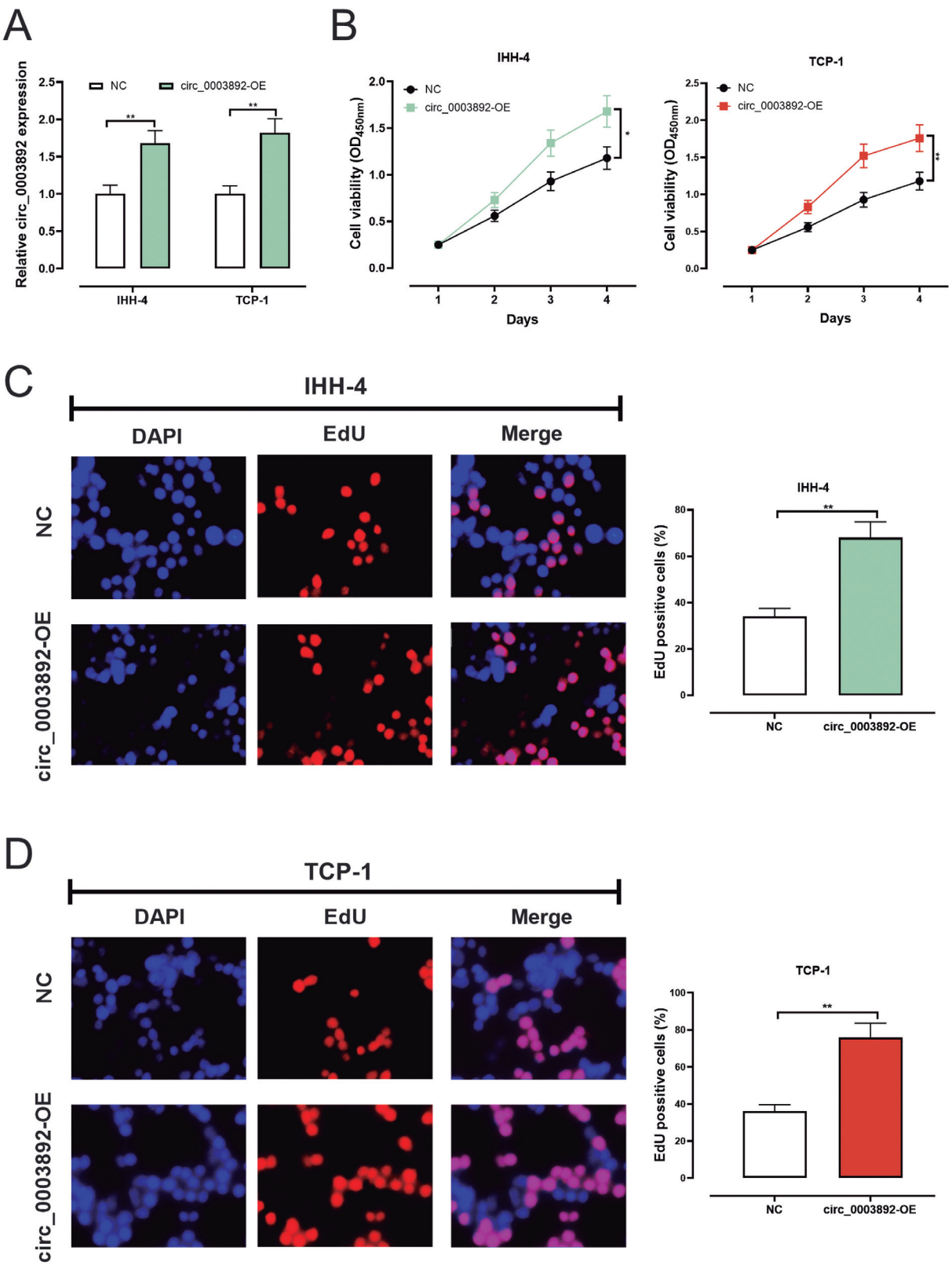

Fig. 2. Circ_0003892 promotes the proliferation of PTC cells. **A.** After transfection of NC or circ_0003892-OE into IHH-4 or TCP-1 cells, the expression of circ_0003892 in IHH-4 or TCP-1 cells was detected by qRT-PCR. **B, C.** The effect of overexpression of circ_0003892 on the proliferation of IHH-1 and TCP-1 cells was detected by CCK-8 and EdU assays. **D.** Transwell assay was used to detect the effect of overexpression of circ_0003892 on the migration and invasion of IHH-1 and TCP-1 cells. All of the experiments were performed in triplicate. **P*<0.05 and ***P*<0.01

function in the development of PTC.

Circ_0003892 promotes the viability, migrative and invasive capabilities of PTC cells

We then transfected IHH-4 and TCP-1 cells with circ_0003892 overexpression plasmid (circ_0003892-OE) or its negative control (NC) to construct an *in vitro* model of high circ_0003892 expression, and qRT-PCR verified that the transfection was successful (Fig. 2A). CCK-8 and EdU assays showed that overexpression of circ_0003892 significantly promoted the proliferation of IHH-4 and TCP-1 cells (Fig. 2B-D). Transwell assay showed that circ_0003892 overexpression promoted the migrative and invasive abilities of PTC cells (Fig. 3A,B). Collectively, circ_0003892 may be a tumor promoter in PTC progression.

Circ_0003892 sponges miR-326 in PTC cells

To expound the molecular mechanism of circ_0003892 in PTC progression, Circinteractome database was searched and a binding site between miR-326 and circ_0003892 was predicted (Fig. 4A). Dual-luciferase reporter gene assay suggested that miR-326 overexpression significantly repressed the luciferase

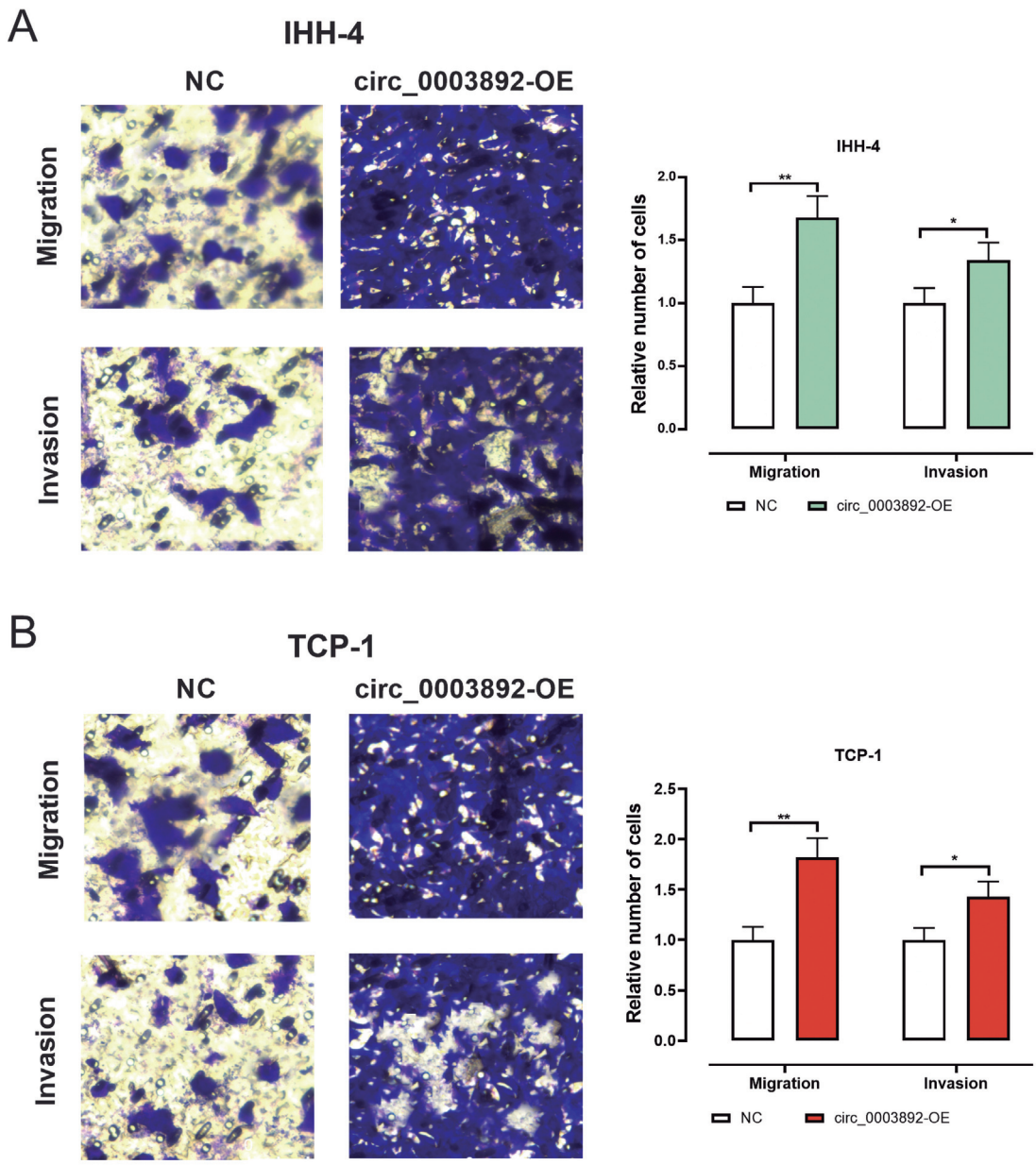

Fig. 3. Circ_0003892 promotes the migration and invasion of PTC cells. **A, B.** Transwell assay was used to detect the effect of circ_0003892 overexpression on the migration and invasion of IHH-1 and TCP-1 cells. All of the experiments were performed in triplicate. **P*<0.05 and ***P*<0.01

activity of circ_0003892 WT, but that of circ_0003892 MUT was not obviously impacted (Fig. 4B). RIP assay showed that both circ_0003892 and miR-326 were significantly enriched in anti-Ago2 group compared with that of the IgG group (Fig. 4C). qRT-PCR showed that miR-326 expression was dramatically inhibited in both PTC tissues and cell lines relative to those in the tissue or human thyroid follicular epithelial cells Nthy-ori 3-1 (Fig. 4D,E). Pearson's correlation analysis suggested that circ_0003892 was negatively correlated with miR-326 expression in PTC tissues (Fig. 4F). These data suggest that circ_0003892 may exert its function by decoying miR-326 in PTC progression.

Circ_0003892 functions by targeting miR-326

To further elucidate the functional relationship between circ_0003892 and miR-326 in PTC, we transfected NC, miR-326 mimics, circ_0003892-OE, and circ_0003892-OE + miR-326 mimics into IHH-4 and TCP-1 cells, respectively. MiR-326 mimics and mim-NC were transfected into IHH-4 and TCP-1 cells respectively, and the efficiency of transfection was verified via qRT-PCR (Fig. 5A). qRT-PCR showed that up-regulation of circ_0003892 inhibited miR-326 expression in IHH-4 and TCP-1 cells, while transfection with miR-326 mimics reversed this effect (Fig. 5B). qRT-PCR showed that transfection of miR-326 mimics promoted miR-326 expression in IHH-4 and TCP-1 cells, while miR-326 mimics had no significant effect on the expression of circ_0003892 (Fig. 5C). CCK-8, EdU and transwell assays showed that the co-transfection of miR-326 mimics greatly alleviated the promoting effect of circ_0003892 overexpression on the growth, migration and invasion of PTC cells (Fig. 5D-F). Collectively, circ_0003892 promotes malignant biological behaviors of PTC cells by targeting miR-326.

Circ_0003892 accelerates PTC progression by targeting the miR-326/LASP1 axis

To elucidate the downstream mechanism of miR-326, TargetScan database was searched, and a binding site between the LASP1 3'-UTR and miR-326 was found

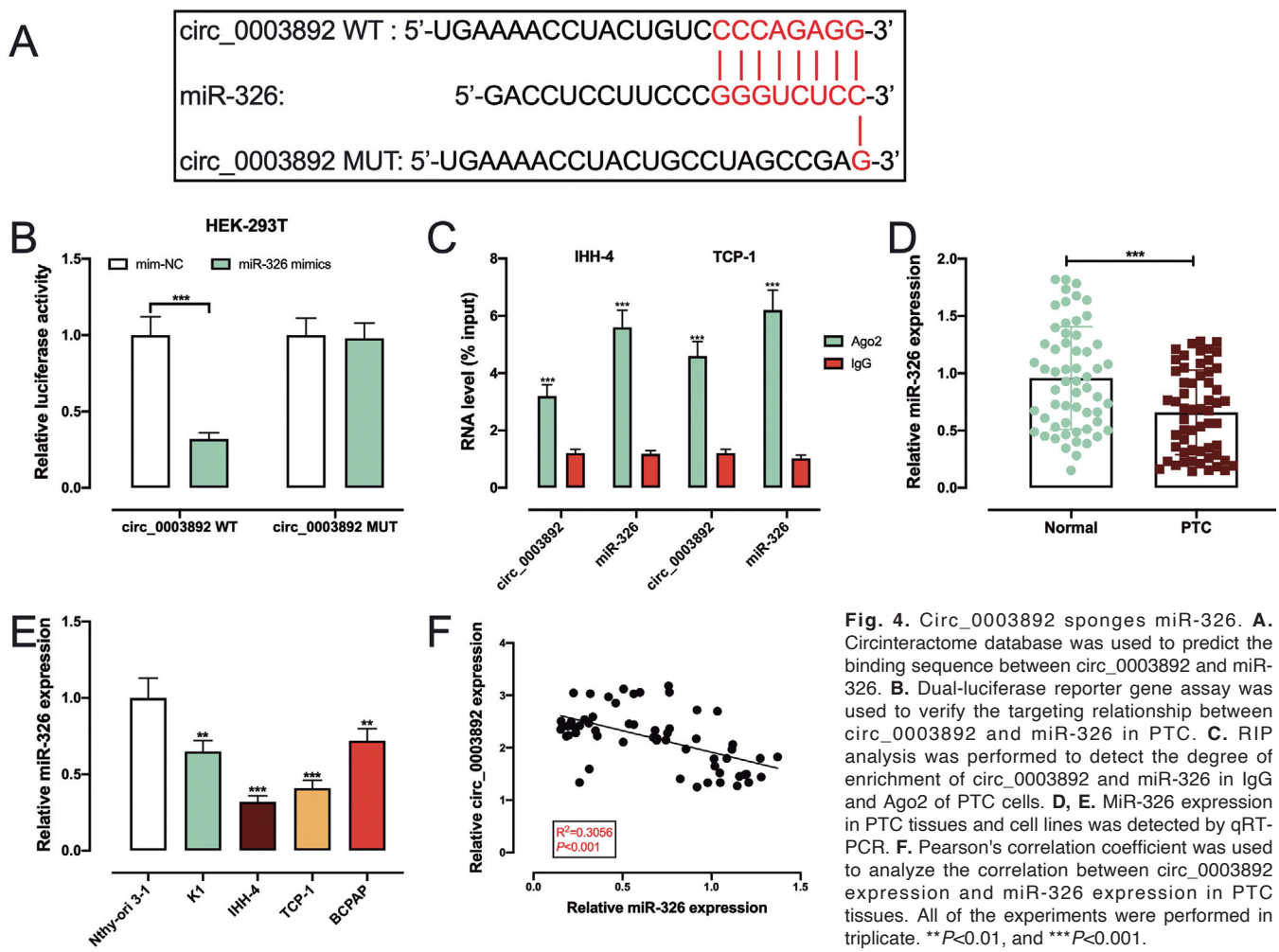

Fig. 4. Circ_0003892 sponges miR-326. **A.** Circinteractome database was used to predict the binding sequence between circ_0003892 and miR-326. **B.** Dual-luciferase reporter gene assay was used to verify the targeting relationship between circ_0003892 and miR-326 in PTC. **C.** RIP analysis was performed to detect the degree of enrichment of circ_0003892 and miR-326 in IgG and Ago2 of PTC cells. **D, E.** MiR-326 expression in PTC tissues and cell lines was detected by qRT-PCR. **F.** Pearson's correlation coefficient was used to analyze the correlation between circ_0003892 expression and miR-326 expression in PTC tissues. All of the experiments were performed in triplicate. ***P*<0.01, and ****P*<0.001.

(Fig. 6A). Dual-luciferase reporter gene assay proved that overexpression of miR-326 significantly inhibited the luciferase activity of LASP1 WT, but had no significant effect on that of LASP1 MUT (Fig. 6B). Up-regulation of circ_0003892 increased LASP1 mRNA and protein expression in IHH-4 and TCP-1 cells, while up-regulation of miR-326 reversed this effect (Fig. 6C,D). qRT-PCR suggested that LASP1 mRNA expression was remarkably up-regulated in PTC tissues compared with that of normal tissues (Fig. 6E). What's more, Pearson's correlation analysis suggested that LASP1 mRNA expression was negatively associated with miR-326 expression, but was positively associated with circ_0003892 expression in PTC tissues (Fig. 6F,G).

Discussion

Increasing numbers of circRNAs have been reported in mammalian cells through high-throughput sequencing technology and bioinformatics (Li et al., 2020). Reportedly, there are many differentially expressed circRNAs in PTC tissues (Lan et al., 2018a,b). As reported, circ_0007694 expression is reduced in PTC tissues, and circ_0007694 overexpression promotes the apoptosis and inhibits the proliferative, migrative and invasive abilities of PTC cells (Long et al., 2020). Circ_0137287 expression is underexpressed in PTC tissues and cell lines, and the low expression of circ_0127287 is associated with aggressive clinicopathological features of PTC, extrathyroid extension, lymph node metastasis, advanced T stage, and larger tumor size, etc. (Lan et al., 2018a,b). In addition, circ_0008274 expression is increased in PTC tissues and cell lines, and circ_0008274 accelerates the growth and invasion of PTC cells via modulating the AMPK/mTOR signaling pathway (Zhou et al., 2018). Here we demonstrated that circ_0003892 expression was raised in PTC tissues and cell lines, which was associated with

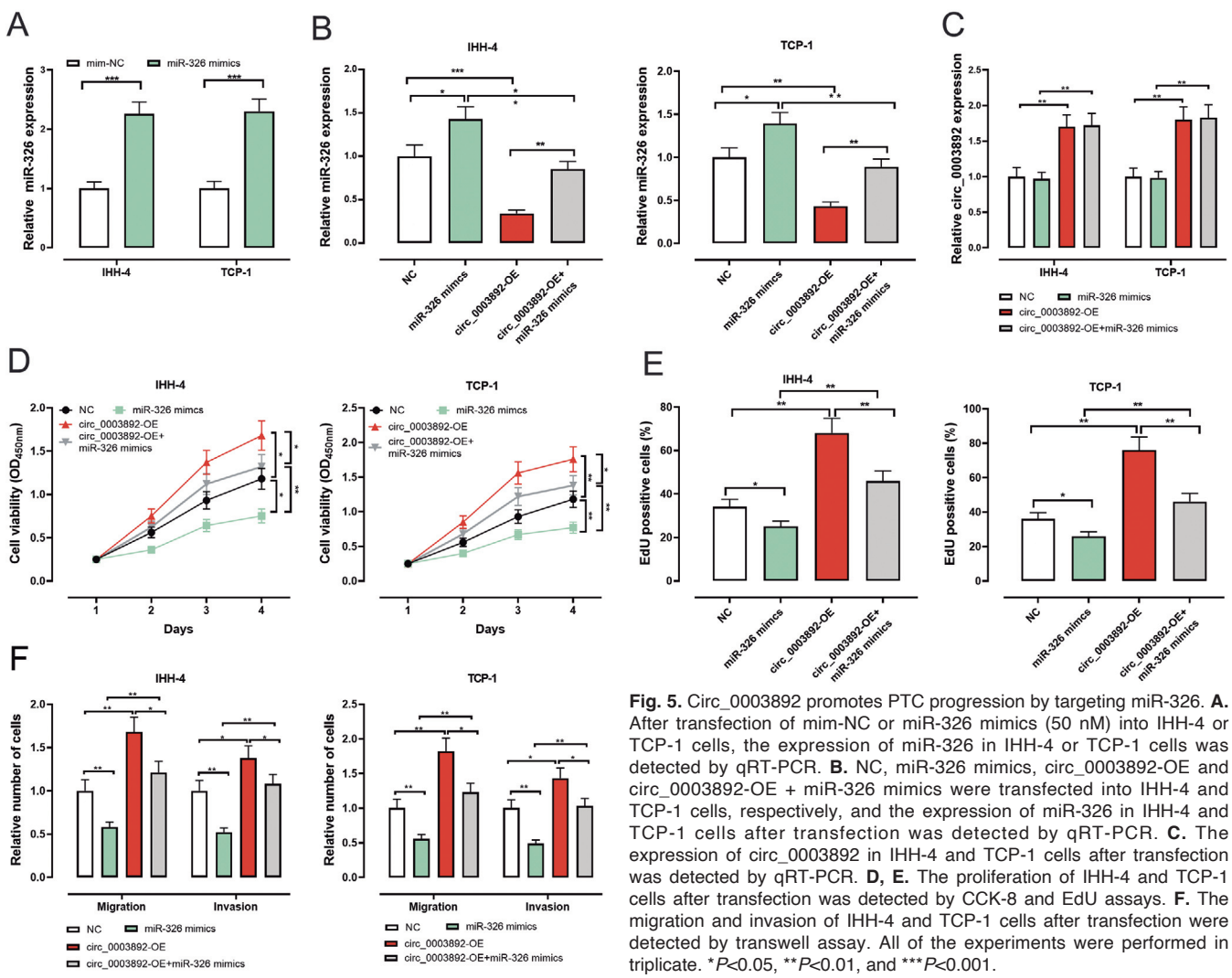

Fig. 5. Circ_0003892 promotes PTC progression by targeting miR-326. **A.** After transfection of mim-NC or miR-326 mimics (50 nM) into IHH-4 or TCP-1 cells, the expression of miR-326 in IHH-4 or TCP-1 cells was detected by qRT-PCR. **B.** NC, miR-326 mimics, circ_0003892-OE and circ_0003892-OE + miR-326 mimics were transfected into IHH-4 and TCP-1 cells, respectively, and the expression of miR-326 in IHH-4 and TCP-1 cells after transfection was detected by qRT-PCR. **C.** The expression of circ_0003892 in IHH-4 and TCP-1 cells after transfection was detected by qRT-PCR. **D, E.** The proliferation of IHH-4 and TCP-1 cells after transfection was detected by CCK-8 and EdU assays. **F.** The migration and invasion of IHH-4 and TCP-1 cells after transfection were detected by transwell assay. All of the experiments were performed in triplicate. **P*<0.05, ***P*<0.01, and ****P*<0.001.

extrathyroidal invasion and larger tumor size in PTC patients. Considering that circRNA is stable and can be easily detected in tumor tissues and body fluids, circ_0003892 is promising to be a biomarker for the diagnosis and prognosis evaluation of PTC patients, which remains to be validated with a larger cohort of patients (Wang et al., 2016). Additionally, we confirmed that circ_0003892 overexpression promoted the proliferative, migrative and invasive abilities of PTC cells. Collectively, circ_0003892 partakes in the progression of PTC and may be a tumor promoter.

MiRNAs have important functions in modulating biological behaviors such as cell growth, differentiation and apoptosis (Wang et al., 2019). MiR-326 is a miRNA that is vital in modulating cancer progression (Liu et al., 2017; Liang et al., 2018; Pan et al., 2019). In prostate cancer tissues, miR-326 expression is inhibited, which is closely associated with poor patient prognosis (Liang et al., 2018). In endometrial cancer, miR-326 expression is reduced and miR-326 can inhibit the viability, migration, invasion, and epithelial-mesenchymal transition of endometrial cancer cells by targeting TWIST1 (Liu et al., 2017). CircRNAs can exert their functions by decoying miRNA (Zhu et al., 2019). For example,

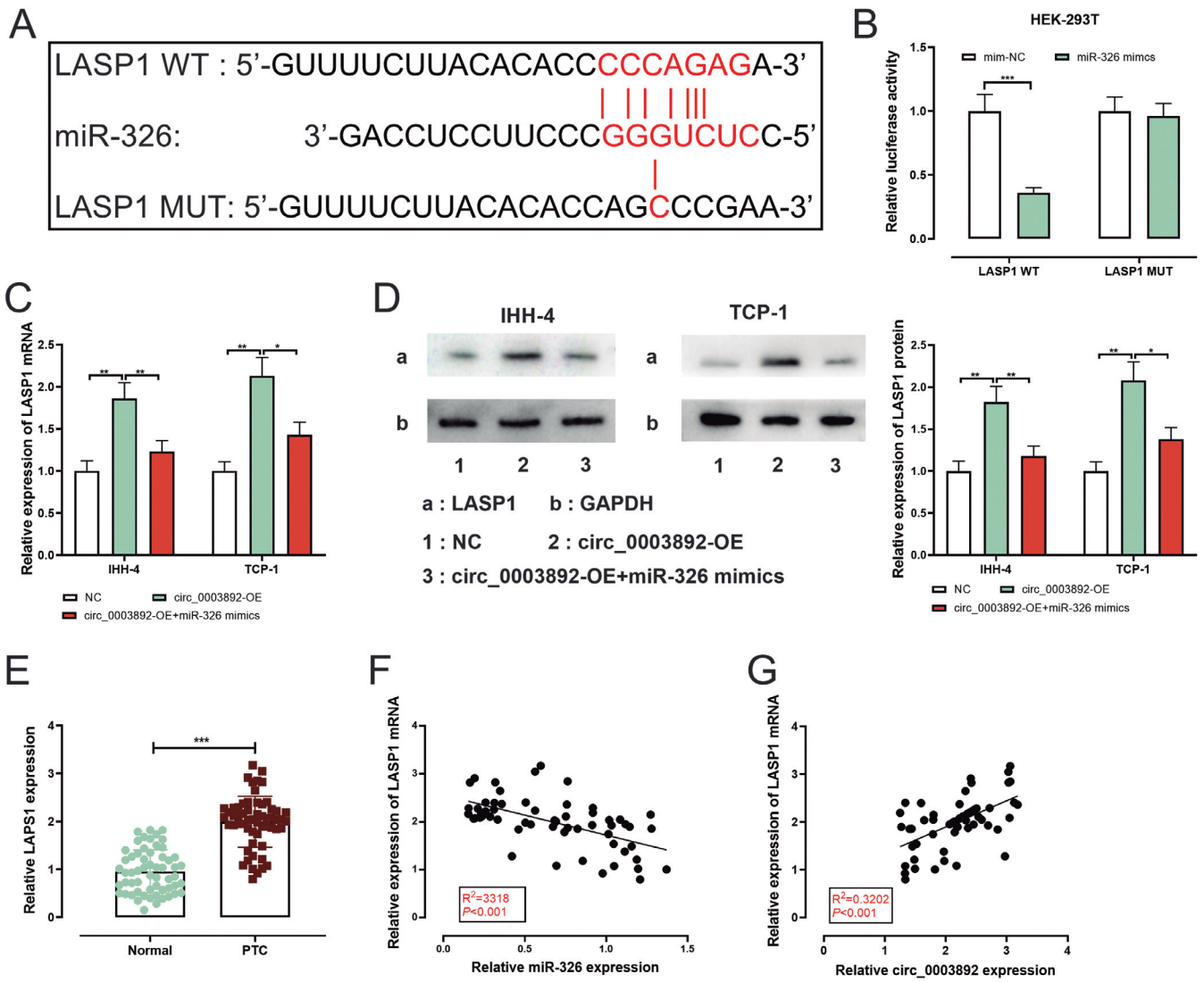

Fig. 6. Circ_0003892 plays a cancer-promoting role by regulating the miR-326/LASP1 axis. **A.** Targetscan database predicted that there was a binding site between miR-326 and LASP1 3'-UTR. **B.** Dual-luciferase reporter gene assay was used to validate the targeting relationship between miR-326 and LASP1 3'-UTR in PTC. **C, D.** LASP1 mRNA expression and protein expression in IHH-4 and TCP-1 cells transfected with circ_0003892 overexpression plasmid or miR-326 mimics alone and cotransfected with circ_0003892 overexpression plasmid and miR-326 mimics were detected by qRT-PCR and western blot, respectively. **E.** The expression of LASP1 mRNA in PTC tissues and normal tissues was detected by qRT-PCR. **F, G.** Pearson's correlation coefficient was used to analyze the correlation between LASP1 mRNA expression and miR-326 expression or circ_0003892 expression in PTC tissues, respectively. All of the experiments were performed in triplicate. **P*<0.05, ***P*<0.01, and ****P*<0.001.

circ_0011290 enhances the viability, growth, and inhibits apoptosis of PTC cell via adsorbing miR-1252 and upregulating FSTL1 expression (Hu et al., 2020). Here we found that circ_0003892 competitively binds with miR-326 and negatively regulates miR-326 expression. We proved that miR-326 overexpression counteracted the promoting effects of circ_0003892 overexpression on the proliferative, migrative and invasive capabilities of PTC cells. These results suggest that circ_0003892 may target miR-326 to promote the progression of PTC.

LIM and SH3 domain-containing proteins, as reported, are elevated in multiple human malignancies and are involved in a wide range of cellular processes, including tumor growth, metastasis and chemoresistance (Zhong et al., 2018). LASP1 was originally screened out from a cDNA library of breast metastases (Mihlan et al., 2013). Although LASP1 protein is lowly expressed in normal human tissues, there is a high expression of LASP1 protein in some types of cancer (such as head and neck squamous cell carcinoma, glioma and PTC) (Gao and Han, 2017; Liu et al., 2018; Chen et al., 2020). In head and neck squamous cell carcinoma, LASP1 expression is upregulated, which is associated with a poor patient prognosis; LASP1 promotes the proliferation, invasion, and colony formation of cancer cells through direct interaction with HSPA1A (Chen et al., 2020). Depletion of LASP1 restrains the viability and migration *in vitro* and tumorigenicity *in vivo* of glioma cells (Liu et al., 2018). In thyroid cancer tissues, LASP1 expression is upregulated, and silencing of LASP1 inhibits the malignancy of thyroid cancer cells (Gao and Han, 2017). In this study, we identified a potential binding site between miR-326 and LASP1 3'-UTR. Furthermore, we confirmed that miR-326 can target LASP1. In addition, circ_0003892 up-regulated LASP1 expression in PTC cells through sponging miR-326. Collectively, the circ_000389/miR-326/LASP1 regulatory axis may be pivotal in the progression of PTC.

In summary, circ_0003892 expression was increased in PTC tissues and cell lines. Mechanistically, circ_0003892 enhanced the proliferative, migrative and invasive abilities of PTC cells by regulating the miR-326/LASP1 axis. Our study identified circ_0003892 as a key circRNA that promotes the development of PTC. Circ_0003892 may be a promising biomarker or therapeutic target, and should be the focus of future studies into the molecular mechanism of PTC progression.

Competing interests. The authors declare that they have no competing interests.

Ethics statement. Our study was approved by the Ethics Review Board of the First Affiliated Hospital of Xi'an Jiaotong University.

Data Availability Statement. The data used to support the findings of this study are available from the corresponding author upon request.

Funding Information. None.

References

Chen L., Heikkinen L., Wang C., Yang Y., Sun H. and Wong G. (2019). Trends in the development of miRNA bioinformatics tools. Brief Bioinform. 20, 1836-1852.

Chen Q., Wu K., Qin X., Yu Y., Wang X. and Wei K. (2020). LASP1 promotes proliferation, invasion in head and neck squamous cell carcinoma and through direct metastasis with HSPA1A. J. Cell Mol. Med. 24, 1626-1639.

Coca-Pelaz A., Shah J.P., Hernandez-Prera J.C., Ghortin R.A., Rodrigo J.P., Hartl D.M., Olsen K.D., Shaha A.R., Zafereo M., Suarez C., Nixon I.J., Randolph G.W., Mäkitie A.A., Kowalski L.P., Vander Poitien V., Sanabria A., Gunas-Lichius O., Simo R., Zbären P., Angelos P., Khafif A., Rinaldo A. and Ferlito A. (2020). Papillary thyroid cancer-aggressive variants and impact on management: A narrative review. Adv. Ther. 37, 3112-3128.

Gao W. and Han J. (2017). Silencing of LIM and SH3 protein 1 (LASP-1) inhibits thyroid cancer cell proliferation and invasion. Oncol. Res. 25, 879-886.

Ge M.H., Cao J., Wang J.Y., Huang Y.Q., Lan X.B., Yu B., Wen Q.L. and Cai XJ. (2017). Nomograms predict specific regional recurrence and distant recurrence of papillary thyroid carcinoma following partial or total thyroidectomy. Medicine (Baltimore) 96, e7575.

Gong J., Kong X., Qi J., Lu J., Yuan S. and Wu M. (2021). CircRNA104565 promoted cell proliferation in papillary thyroid carcinoma by sponging miR-134. Int. J. Gen. Med. 14, 179-185.

Haugen B.R., Alexander E.K., Bible K.C., Doherty G.M., Mandel S.J., Nikiforov Y.E., Pacini F., Randolph G.W., Sawka A.M., Schlumberger M., Schuff K.G., Sherman S.I., Sosa J.A., Steward D.L., Tuttle R.M. and Wartofsky L. (2016). 2015 American thyroid management guidelines for adult patients with thules noderger and differentiated thyroid cancer: The american thyroid association guidelines task force on thyroid nodules and differentiated thyroid cancer. Thyroid 26, 1-133.

Hu Z., Zhao P., Zhang K., Zang L., Liao H. and Ma W. (2020). Hsacirc0011290 regulates signal proliferation, apoptosis and glycolytic phenotype in papillary thyroid cancer via miR- 1252/FSTL1 pathway. Arch. Biochem. Biophys. 685, 108353.

Jin J., Zhang J., Xue Y., Luo L., Wang S. and Tian H. (2019). miRNA-15a regulates the proliferation and apoptosis of papillary thyroid carcinoma via regulating AKT pathway. Onco. Targets Ther. 12, 6217-6226.

Krol J., Loedige I. and Filipowicz W. (2010). The widespread regulation of microRNA biogenesis, function and decay. Nat. Rev. Genet. 11, 597-610.

Lan X., Cao J., Xu J., Chen C., Zheng C., Wang J., Zhu X., Zhu X. and Ge M. (2018a). Decreased expression of hsacirc0137287 predicts aggressive clinicopathologic characteristics in papillary thyroid carcinoma. J. Clin. Lab. Anal. 32, e22573.

Lan X., Xu J., Chen C., Zheng C., Wang J., Cao J., Zhu X and Ge M. (2018b). The landscape of circular RNA expression profiles in papillary thyroid carcinoma based on RNA sequencing. Cell Physiol. Biochem. 47, 1122-1132.

Li Y., Hu J., Li L., Cai S., Zhang H., Zhu X., Guan G. and Dong X. (2018). Upregulated circular RNA 0016760 unfavorable prognosis circin NSCLC and promotes cell progression through miR-1287/GAGE1 axis. Biochem. Biophys. Res. Commun. 503, 2089-2094.

Li R., Jiang J., Shi H., Qian H., Zhang X. and Xu W. (2020). CircRNA: a

rising star in gastric cancer. Cell Mol. Life Sci. 77, 1661-1680.

Liang X., Li Z., Men Q., Li Y,. Li H. and Chong T. (2018). miR-326 functions as a tumor suppressor in human prostatic carcinoma by targeting Mucin1. Biomed. Pharmacother. 108, 574-583.

Liu W., Zhang B., Xu N., Wang M.J. and Liu Q. (2017). miR-326 regulates EMT and metastasis of endometrial cancer through targeting TWIST1. Eur. Rev. Med. Pharmacol Sci. 21, 3787-3793.

Liu W., Zhao J., Jin M. and Zhou M. (2019). circRAPGEF5 contributes to papillary thyroid proliferation and metastatis by regulation miR-198/FGFR1. Mol. Ther. Nucleic Acids 14, 609-616.

Liu Y., Gao Y., Li D., He L., Iw L., Hao B., Chen X. and Cao Y. (2018). LASP1 negatively promotes glioma cell proliferation and migration and is regulated by miR-377-3p. Biomed. Pharmacother. 108, 845-851.

Long M.Y., Chen J.W., Zhu Y., Luo D.Y., Lin S.J., Peng X.Z., Tan L.P. and Li H.H. (2020). Comprehensive circular RNA profiling reveals the regulatory role of circRNA 0007694 in papillary thyroid carcinoma. Am. J. Transl. Res. 12, 1362-1378.

Mihlan S., Reiß C., Thalheimer P., Herterich S., Gaetzner S., Kremerskothen J., Pavenstädt H.J., Lewandrowski U., Sickmann A. and Butt E. (2013). Nuclear phosphorylation of LASP-1 is regulated by import and dynamic protein-phosphorylation interactions. Oncogene 32, 2107-2113.

Nie F.R., Li Q.X., Wei H.F. and Ma Y. (2020). miR-326 inhibits the progression of papillary thyroid carcinoma by targeting MAPK1 and ERBB4. Neoplasma 67, 604-613.

Pan Y.J., Wan J. and Wang C.B. (2019). MiR-326: Promising biomarker for cancer. Cancer Manag. Res. 11, 10411-10418.

Patop I.L., Wüst S. and Kadener S. (2019). Past, present, and future of circRNAs. EMBO J. 38, e100836.

Svoronos A.A., Engelman D.M. and Slack F.J. (2016). OncomiR or tumor suppressor? the duplicity of MicroRNAs in cancer. Cancer Res. 76, 3666-3670.

Wang F., Nazarali A.J. and Ji S. (2016). Circular RNAs as potential biomarkers for cancer diagnosis and therapy. Am. J. Cancer Res. 6, 1167-1176.

Wang J., Liu S., Li J., Zhao S. and Yi Z. (2019). Roles for miRNAs in osteogenic differentiation of bone marrow mesenchymal stem cells. Stem Cell Res. Ther. 10, 197.

Yao Y., Chen X., Yang H., Chen W., Qian Y., Yan Z., Liao T., Yao W., Wu W., Yu T., Chen Y. and Zhang Y. (2019). Hsacirc0058124 papillary cancer tumorigenesis and invasiveness through the NOTCH3/thyroid GATAD2A axis. J. Exp. Clin. Cancer Res. 38, 318.

Yin Y., Hong S., Yu S., Huang Y., Chen S., Liu Y., Zhang Q., Li Y. and Xiao H. (2017). MiR-195 inhibits tumor growth and metastasis in papillary thyroid carcinoma cell lines by targeting CCND1 and FGF2. Int. J. Endocrinol. 2017, 6180425.

Zhong C., Chen Y., Tao B., Peng L., Peng T., Yang X., Xia X. and Chen L. (2018). LIM and SH3 protein 1 cell growth and chemosensitivity of human glioblastoma via the PI3K/AKT pathway. BMC Cancer 18, 722.

Zhou G.K., Zhang G.Y., Yuan Z.N., Pei R. and Liu D.M. (2018). Hascirc0008274 promotes cell proliferation and invasion involving AMPK/mTOR signaling pathway in papillary thyroid carcinoma. Eur. Rev. Med. Pharmacol. Sci. 22, 8772-8780.

Zhu J., Zhang X., Gao W., Hu H., Wang X. and Hao D. (2019). LncRNA/circRNA miRNA mRNA ceRNA network in lumbar intervertebral disc degeneration. Mol. Med. Rep. 20, 3160-3174.

Accepted November 17, 2022